imental error with the data reported graphically by Griskey et al. (8).

Correlation of Second Virial Coefficients

We have compared our data with second virial coefficients predicted by the Tsonopoulous (1) modification of the Pitzer-Curl correlation. For nonpolar gases, the Tsonopoulos-Pitzer-Curl correlation is

$$BZ_c/V_c = f^{(0)} + \omega f^{(1)} \quad (1)$$

where

$$f^{(0)} = 0.1445 - 0.330/T_R - 0.1385/T_R^2 - 0.0121/T_R^3 - 0.000607/T_R^8 \quad (2)$$

$$f^{(1)} = 0.0637 + 0.331/T_R^2 - 0.423/T_R^3 - 0.008/T_R^8 \quad (3)$$

and ω is Pitzer's acentric factor. The second virial coefficient B of any gas may thus be predicted from a knowledge of its critical properties and acentric factor.

The correlation may be extended to mixtures via the van der Waals one-fluid model whereby the pure-component properties T_c, V_c, Z_c, and ω are replaced by the pseudocritical values T_{cm}, V_{cm}, Z_{cm}, and ω_m as follows:

$$T_{cm}V_{cm} = \sum_i \sum_j x_i x_j T_{cij} V_{cij} \quad (4)$$

$$V_{cm} = \sum_i \sum_j x_i x_j V_{cij} \quad (5)$$

$$Z_{cm} = \sum_i x_i Z_{ci} \quad (6)$$

$$\omega_m = \sum_i x_i \omega_i \quad (7)$$

The van der Waals one-fluid model has been used with considerable success in extending equations of state to mixtures (see, for example, ref 9). The like terms (i = j) are obtained from pure-component properties, whereas the unlike terms (i ≠ j) must be obtained from the properties of the binary mixtures. The usual prescription is to write

$$T_{cij} = \xi_{ij}(T_{ci}T_{cj})^{1/2} \quad (8)$$

$$T_{cij} = \{1/2(V_{ci}^{1/3} + V_{cj}^{1/3})\}^3 \quad (9)$$

where the binary interaction coefficient ξ_{ij} is obtained from binary-mixture properties. No further information is required to predict the properties of ternary and higher mixtures.

We have used the van der Waals one-fluid model together with the Lorentz-Berthelot mixture prescription (eq 8 and 9) and the Tsonopoulos-Pitzer-Curl equations to correlate second virial coefficients of the five propane-isomeric hexane systems. The results are summarized in Table VI. As can be seen, good agreement between prediction and experiment can be obtained with $\xi_{ij} = 1.0$ on all cases. On the whole, agreement appears to be within the experimental error of the data. It would therefore appear that the effect of size on the second virial coefficient is more important than the effect of the shape of the molecules and that this effect can be adequately represented by the Tsonopoulos-Pitzer-Curl equation and the van der Waals one-fluid model.

Table VI. Comparison of Calculated and Experimental Second Virial Coefficients of Propane-Isomeric Hexane Mixtures ($\xi_{ij} = 1.0$ Throughout)

system	no. of data	av abs deviation, %	max deviation, %
propane + *n*-hexane	40	5.0	11.7
propane + 2-methylpentane	38	2.7	7.3
propane + 3-methylpentane	39	2.4	6.5
propane + 2,2-dimethylbutane	37	3.7	10.8
propane + 2,3-dimethylbutane	34	4.9	9.6

Glossary

B	second virial coefficient
f	functions in eq 1
T	thermodynamic temperature
V	volume
x	mole fraction
Z	compressibility
ω	acentric factor
ξ	binary interaction coefficient

Subscripts

c	critical
i, j	components i and j
m	mixture value
R	reduced value

Literature Cited

(1) Tsonopoulos, Constantine *AIChE J.* **1974**, *20*, 263.
(2) Hayden, J. G.; O'Connel, J. P. *Ind. Eng. Chem. Process Des. Dev.* **1975**, *14*, 209.
(3) Tarakad, R. R.; Danner, R. P. *AIChE J.* **1977**, *23*, 685.
(4) Kay, W. B.; Rambosek, G. M. *Ind. Eng. Chem.* **1953**, *45*, 221.
(5) Jones, A. E.; Kay, W. B. *AIChE J.* **1967**, *13*, 717, 720.
(6) Chun, S. W. Ph.D. Thesis, The Ohio State University, Columbus, OH, 1964.
(7) McGlashan, M. L.; Potter, D. J. B., *Proc. R. Soc. London, Ser. A* **1962**, *267*, 478.
(8) Griskey, R. G.; Canjar, L. N.; Stuewe, C. W. *J. Chem. Eng. Data* **1963**, *8*, 341.
(9) Teja, A. S.; Patel, N. C.; Ng, N. H. *Chem. Eng. Sci.* **1978**, *33*, 623.

Received for review October 27, 1980. Accepted January 21, 1981.

Ternary Liquid–Liquid Equilibrium Data for the Cyclohexane–Cyclohexene–Ammonia System

Kiyoharu Ishida, Katsuji Noda,* and Osamu Morinaga

Department of Chemical Engineering, Shizuoka University, Hamamatsu 432, Japan

Ternary liquid–liquid equilibrium data for the cyclohexane–cyclohexene–ammonia system are measured at 0, 20, 30, and 40 °C and are correlated by the Othmer–Tobias and other plots.

Introduction

Liquid–liquid equilibrium data are useful for the design of liquid extraction processes and have been measured or correlated by many authors. Liquid ammonia has good solvency and se-

0021-9568/81/1726-0303$01.25/0

Table I. Liquid-Liquid Equilibrium Data (Weight Fraction) for the Cyclohexane (A)-Cyclohexene (C)-Ammonia (B) System

raffinate layer			extract layer		
X_{AA}	X_{CA}	X_{BA}	X_{AB}	X_{CB}	X_{BB}
		0 °C			
0.979	0.0	0.021	0.032	0.0	0.968
0.874	0.104	0.022	0.029	0.006	0.965
0.653	0.322	0.025	0.023	0.019	0.958
0.472	0.500	0.028	0.017	0.033	0.950
0.329	0.639	0.032	0.012	0.044	0.944
0.172	0.790	0.038	0.006	0.059	0.935
0.0	0.954	0.046	0.0	0.084	0.916
		20 °C			
0.960	0.0	0.040	0.058	0.0	0.942
0.868	0.089	0.043	0.051	0.012	0.937
0.671	0.280	0.049	0.040	0.038	0.922
0.591	0.357	0.052	0.036	0.051	0.913
0.493	0.450	0.057	0.030	0.066	0.904
0.390	0.548	0.062	0.024	0.083	0.893
0.256	0.674	0.070	0.016	0.105	0.879
0.111	0.807	0.082	0.007	0.137	0.856
0.0	0.906	0.094	0.0	0.178	0.822
		30 °C			
0.944	0.0	0.056	0.082	0.0	0.918
0.859	0.083	0.058	0.076	0.014	0.910
0.720	0.217	0.063	0.067	0.041	0.892
0.633	0.301	0.066	0.061	0.058	0.881
0.529	0.401	0.070	0.053	0.080	0.867
0.415	0.510	0.075	0.044	0.107	0.849
0.369	0.554	0.077	0.040	0.120	0.840
0.218	0.691	0.091	0.026	0.170	0.804
0.172	0.731	0.097	0.021	0.187	0.792
0.132	0.765	0.103	0.017	0.206	0.777
0.082	0.805	0.113	0.011	0.227	0.762
0.0	0.851	0.149	0.0	0.276	0.724
		40 °C			
0.919	0.0	0.081	0.118	0.0	0.882
0.871	0.047	0.082	0.116	0.012	0.872
0.803	0.111	0.086	0.110	0.030	0.860
0.637	0.268	0.095	0.098	0.076	0.826
0.571	0.330	0.099	0.094	0.097	0.809
0.485	0.410	0.105	0.088	0.129	0.783
0.478	0.416	0.106	0.087	0.134	0.779
0.394	0.491	0.115	0.081	0.169	0.750
0.284	0.583	0.133	0.073	0.235	0.692
0.244	0.614	0.142	0.069	0.268	0.663
0.194	0.643	0.163	0.065	0.314	0.621
0.130	0.660	0.210	0.059	0.391	0.550
0.115	0.658	0.227	0.058	0.416	0.526

lectivity for separating mixtures of aromatic and paraffinic hydrocarbons (*1*).

In this investigation, ternary liquid–liquid equilibrium data for the cyclohexane–cyclohexene–ammonia system are measured at 0, 20, 30, and 40 °C.

Experimental Section

Ternary liquid–liquid equilibrium data were determined by a slightly modified version of the method reported in the previous paper (*3*). The heterogeneous liquid sample in the equilibrium cell was placed in a constant temperature bath regulated within the range of ±0.03 °C. After equilibrium was reached, an aliquot of each layer was withdrawn in a sampling receiver and the ammonia content was determined titrimetrically. The composition ratio of the organic components was determined by gas chromatography. A 1.5-m column filled with $\beta\beta'$-ODPN was used.

Liquid ammonia was purified from a commercial product by carefully distilling at least three times under pressure so as not to contaminate with trace water. Commercially available guaranteed reagent grade cyclohexane and cyclohexene were further purified by distillation and the constant temperature fraction was used. The boiling points of cyclohexane and cyclohexene are 80.7 and 82.8 °C, respectively.

An analysis of the experimental uncertainties is estimated to be ±0.1% in ammonia and those for the organic compounds are larger than ammonia by one order of magnitude.

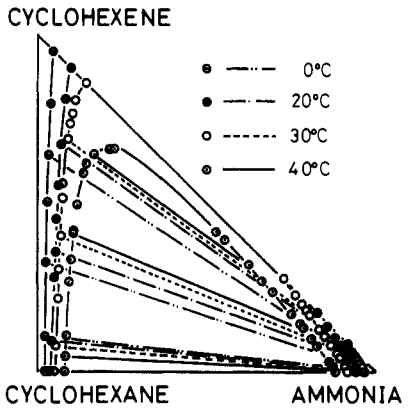

Figure 1. Liquid–liquid equilibrium for the cyclohexane–cyclohexene–ammonia system.

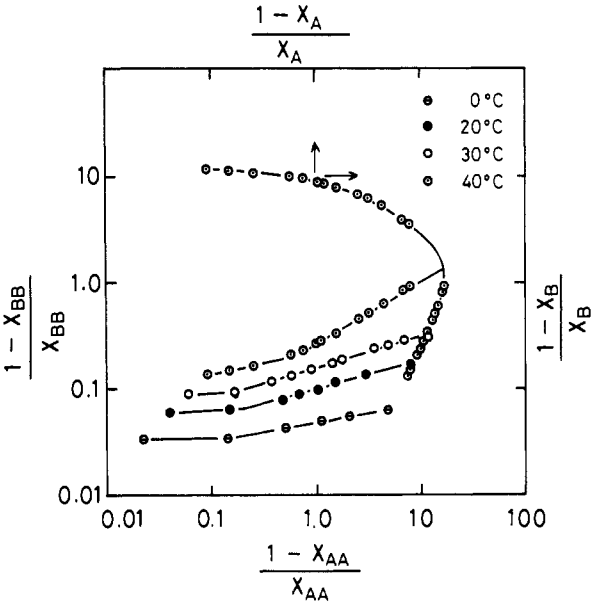

Figure 2. Othmer–Tobias correlation.

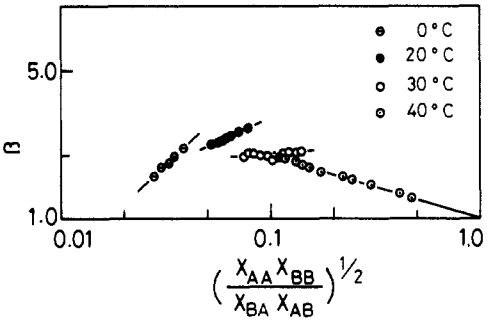

Figure 3. Correlation of β vs. $(X_{AA}X_{BB}/X_{BA}X_{AB})^{1/2}$.

Results and Discussion

The experimental results are given in Table I and are shown in Figure 1. The critical solution temperature for the cyclohexene–ammonia system is 37.8 °C (*4*). Therefore, the ternary solubility curve at 40 °C is type I and the others are type II. In Figure 2, tie lines are plotted on Othmer–Tobias coordinates (*5*). The solubility curve at 40 °C is simultaneously plotted on

the same coordinates. Figure 3 shows plots of the selectivity $\beta_{C,A} = X_{CB}X_{AA}/X_{AB}X_{CA}$ vs. $x_2/x_1 = (X_{AA}X_{BB}/X_{BA}X_{AB})^{1/2}$. (The physical meaning of x_2/x_1 is discussed in ref 2.) The dependence of the solubility on temperature is shown clarly in these figures.

Glossary

X_{AB}	liquid weight fraction of A in the B-rich phase
x_2/x_1	the quantity defined by $(X_{AA}X_{BB}/X_{BA}X_{AB})^{1/2}$
$\beta_{C,A}$	selectivity of B for C from an A-C solution

Subscripts

A	component (diluent, cyclohexane)
B	component (solvent, ammonia)
C	component (solute, cyclohexene)

Literature Cited

(1) Ishida, K. *Bull. Chem. Soc. Jpn.* **1957**, *30*, 512.
(2) Ishida, K. *J. Chem. Eng. Data* **1961**, *6*, 489.
(3) Ishii, K.; Hayami, S.; Shirai, T.; Ishida, K. *J. Chem. Eng. Data* **1966**, *11*, 288.
(4) Noda, K.; Fukawa, K.; Yanagisawa, M.; Ishida, K. *Kagaku Kogaku* **1971**, *35*, 245.
(5) Othmer, D. F.; Tobias, P. F. *Ind. Eng. Chem.* **1942**, *34*, 690.

Received for review October 30, 1980. Accepted February 24, 1981.

Vapor–Liquid Equilibria of the Water–Ethanol System at Low Alcohol Concentrations

Juan Hong,*† Michael R. Ladisch,‡ and George T. Tsao§

Purdue University, West Lafayette, Indiana 47907

Vapor–liquid equilibrium data for the ethanol–water system at 760 mmHg are collected by using a Gillespie-type still. Data in the range of ethanol concentration from 0.01 to 1.0 wt % are scarce, and yet they are much needed in the design of efficient ethanol recovery systems.

There has been strong interest in the use of renewable energy to reduce the consumption of petroleum fuel. An important consideration in biomass conversion concerns the energy consumption needed to produce alcohol compared to the energy content of the final alcohol product. Hence, there is a special interest in reducing energy consumption in the ethanol recovery step since it consumes a significant portion of the energy of the overall process. In low-energy distillation modeling, the bottom product stream is often assumed to contain no more than 0.02 wt % ethanol (*1*, *2*). This constraint implies the requirement of efficient stripping. Otherwise, this alcohol loss becomes a significant cost factor when the feed concentration is low. In fact, low alcohol concentrations of 6–8 wt % ethanol are commonly encountered in the fermentation beer stream fed to a distillation system in the manufacture of fuel alcohol. How one can recover alcohol from a very dilute aqueous solution has thus became increasingly important as the interest in fuel alcohol further develops.

Approximately 80 reports have appeared in the literature since 1895 on the vapor–liquid equilibrium data of the ethanol–water system (*3*). However, these investigations have seldom been performed at concentrations lower than 1 wt % ethanol. Specifically, only the report by Dalager (*4*) contains data at concentrations between 0.01 and 0.1 wt % ethanol (four data points with concentrations between 0.038 and 0.053 wt % ethanol). In this paper, extensive vapor–liquid equilibrium data are reported for ethanol concentrations of 0.01–1.0 wt %.

†Laboratory of Renewable Resources Engineering, A. A. Potter Engineering Center.
‡Laboratory of Renewable Resources Engineering, A. A. Potter Engineering Center; Department of Agricultural Engineering; and School of Chemical Engineering.
§Laboratory of Renewable Resources Engineering, A. A. Potter Engineering Center; and School of Chemical Engineering.

Experimental Methods and Materials

Apparatus. An equilibrium still designed on the principle of the Gillespie still (*5*) was used. Figure 1 shows the apparatus, which was built mainly of Pyrex glass and consisted of a mixture reservoir, a still, a disengagement vessel, a condensate collector, and a cottrell tube connecting the disengagement vessel to the still. The still is a concentric tube surrounded by heating tape. The boiling rate of the mixture in the outer shell of the tube was controlled by heat input through the heating tape. The cottrell tube and the disengagement vessel were insulated from the surroundings by glass wool. The tip of the thermocouple in the disengagement vessel was located at the end of the cottrell tube. To prevent condensation of the atmospheric moisture through the condenser, a Drierite container was attached to the condenser.

All experiments were run at atmospheric pressure (760 mmHg). The temperatures were measured with an alumel–chromel thermocouple and displayed on a digital thermometer (Omega Engineering, Inc., Stamford, CT 06907). The measurements were made to 0.2 °C accuracy. The determinations of the ethanol concentrations were done by gas chromatography, refractive index, or a Karl Fischer-type water analyzer depending on the concentration range. The concentrations in the range of 0.01~2 wt % were measured by gas chromatography (Model 311, Carle Instruments, Inc., Anaheim, CA 92801) equipped with a flame ionization detector (FID) and a thermal conductivity detector (TCD). The concentrations in the range of 2~20 wt % were measured by a refractometer (Abbe 3L, Baucsh & Lomb, Rochester, NY 14625). The concentrations above 20 wt % were determined by a Karl Fischer water analyzer (Aquatest-IV, Photovolt Corp., New York, NY 10010). The column (stainless, 87 cm long, 0.635 cm o.d, 0.319 cm i.d) used for gas chromatography was packed with pure cellulose (Avicel PH-101, Lot 1645, FMC Corp., Marcus Hook, PA 19061) which is capable of the separation of ethanol and water (*6*). The column was thermostated at 150 °C in an oven. Helium, hydrogen, and air were used as carrier gas, fuel,

0021-9568/81/1726-0305$01.25/0